Journal of Power Sources 195 (2010) 4098–4103

Contents lists available at ScienceDirect

Journal of Power Sources

journal homepage: www.elsevier.com/locate/jpowsour

Enhanced long-term durability of proton exchange membrane fuel cell cathode by employing Pt/TiO_2/C catalysts

Xin Liu[a,b], Jian Chen[a,*], Gang Liu[a,b], Li Zhang[a,b], Huamin Zhang[a], Baolian Yi[a]

[a] PEMFC Key Materials and Technology Laboratory, Dalian Institute of Chemical Physics, Chinese Academy of Sciences, Zhongshan Road 457#, Dalian 116023, PR China
[b] Graduate University of the Chinese Academy of Sciences, Beijing 100039, China

ARTICLE INFO

Article history:
Received 18 January 2010
Accepted 27 January 2010
Available online 4 February 2010

Keywords:
Carbon–titanium dioxide support platinum
Cathode catalyst
Proton exchange membrane fuel cell
Long-term durability

ABSTRACT

Pt/TiO_2/C catalysts are employed as the cathode catalysts for proton exchange membrane fuel cell (PEMFC). The comparative studies on the Pt/C and Pt/TiO_2/C catalysts are conducted with the physical and electrochemical techniques.

After the accelerating aging test (AAT), the remaining electrochemical active surface area (EAS) of the Pt/TiO_2/C catalysts is 75.6%, which is larger than that of the Pt/C catalysts (42.6%). The apparent exchange current density (i^0_{app}) of the oxygen reduction reaction (ORR) at the Pt/C catalysts decreases from 3.02×10^{-9} to 1.32×10^{-11} A cm^{-2} after the AAT. And the value of i^0_{app} of the ORR at the Pt/TiO_2/C catalysts is 2.88×10^{-9} A cm^{-2} before the AAT and 2.51×10^{-9} A cm^{-2} after the AAT. Furthermore, the output performance degradation of the PEMFC using the Pt/TiO_2/C cathode catalysts is also less than that using the Pt/C catalysts. The particle size of the Pt/C catalysts increases significantly from 5.3 to 26.5 nm after the AAT. The mean particle size of the Pt/TiO_2/C catalysts is 7.3 nm before the AAT and 9.2 nm after the AAT. It can be concluded that the long-term durability of the Pt/TiO_2/C catalysts in a PEMFC is much better than that of the Pt/C catalysts.

1. Introduction

Proton exchange membrane fuel cell (PEMFC) is a kind of potential alternative power source for transport applications [1]. One of the main obstacles for the application of PEMFC in vehicles is the long-term durability of the cathode catalysts, especially when the fuel cells are operated under the cycle duty. Currently, the carbon-supported platinum (Pt/C) is still the most widely used electro-catalyst in PEMFC. The degradation of Pt/C cathode catalysts results from both the reduction of electrochemical active surface area (EAS) of Pt [2] and the corrosion of carbon support [3]. These two factors are influenced and accelerated by each other [4–6]. The Pt agglomeration [7,8] caused by the dissolution/re-deposition [9,10] of the Pt and the transfer of the Pt atoms at the surface of carbon support [2] is considered to be the main reason for the reduction of the catalyst activity.

The agglomeration of Pt particles can be hindered effectively by alloying the Pt with the non-precious metal. The Pt alloy catalysts have been prepared and served as the PEMFC cathode catalysts. Besides the high catalytic activity, the stability of the carbon-supported Pt alloy catalysts is also better than the Pt/C catalysts [11–13]. It is indicated that the improved durability is attributed to the "anchor effects" of the non-precious metal to the Pt at the carbon surface, which makes the Pt atom to insert or anchor at the surface of carbon more stably. However, the dissolution of the non-alloyed metal may accelerate the degradation of the membrane and decrease the surface of Pt which is crucial to the catalytic activity towards ORR [10]. Furthermore, the output performance of PEMFC will be reduced. These issues have made many of the alloy compositions impractical [14–20]. Therefore, to develop more durable cathode catalysts for PEMFC is still a challenge.

Recently, transition metal oxides, such as ZrO_2, have been applied to improve the long-term durability of the carbon-supported platinum catalysts on the basis of the strong metal–support interaction and the anchor effect between the metal oxides and the adjacent Pt atoms [21,22]. TiO_2 is highly stable in acidic environment [23,24]. The Pt/TiO_2/C catalysts have been employed as the cathode catalyst in both PEMFC [25] and direct methanol fuel cell (DMFC) [26]. It was reported that the electrochemical active surface area (EAS) of the platinum in the catalyst was increased with the addition of TiO_2 due to the synergistic effects of the interface between Pt and TiO_2 and the spillover of hydrogen [25]. Besides, the TiO_2 films thinner than 18 nm were found to be proton-

* Corresponding author. Tel.: +86 13940971209; fax: +86 41184665057.
E-mail address: chenjian@dicp.ac.cn (J. Chen).

0378-7753/$ – see front matter © 2010 Elsevier B.V. All rights reserved.
doi:10.1016/j.jpowsour.2010.01.077

conducting [27,28]. In addition, the tolerance of the cathode to the methanol permeating from the anode via Nafion membrane in a DMFC was obviously enhanced by introducing TiOx in the catalyst [26]. However, the long-term durability of $Pt/TiO_2/C$ when it is employed as PEMFC cathode catalyst has not been investigated yet.

In this paper, $Pt/TiO_2/C$ catalyst was prepared and employed as the cathode catalyst for PEMFC. The comparison of the long-term durability of $Pt/TiO_2/C$ and Pt/C catalysts was conducted with in situ and ex situ measurement by evaluating the single cell performance, cyclic voltammetry (CV) curve and steady-state polarization curve. Meanwhile, the morphological changes of the cathode catalysts caused by the accelerating aging test (AAT) were investigated by transmission electron microscope (TEM).

2. Experimental

2.1. Preparation of catalysts

$Pt/TiO_2/C$ catalyst (Pt content was 40 wt.%) was prepared with a two-step reaction method. Ti-2triethanolamine (Ti-2TEA) was firstly prepared by using $Ti(OBu)_4$ as the precursor. The carbon-supported TiO_2 (TiO_2/C) was prepared by mixing Ti-2TEA with a suspension of Vulcan XC-72. The Pt metal was chemically reduced from H_2PtCl_6 in ethylene glycol (EG) solution and deposited on TiO_2/C powders. Afterwards, the compositions were heat-treated at 500 °C in N_2 for 3 h to obtain $Pt/TiO_2/C$ catalyst. The content of Pt and Ti in the catalyst was detected by inductively coupled plasma (ICP).

For comparison, Pt/C catalyst (Pt content was 40 wt.%) was prepared with the EG method.

2.2. Preparation of membrane electrode assembly (MEA) and PEMFC single cell

The gas diffusion electrodes consisting of gas diffusion layer and catalyst layer were prepared with the procedure described elsewhere [29]. The gas diffusion layer with a micro-porous layer (MPL) was prepared by coating a mixture of Vulcan XC-72 carbon black and PTFE (30 wt.% in dry state) onto a waterproofed carbon paper and was heated at 240 °C for 30 min, and then was calcined at 340 °C for 30 min. The catalyst layer was prepared by spraying a mixture containing a certain amount of home-made Pt/C or $Pt/TiO_2/C$ catalysts, 10 wt.% PTFE and ethanol onto the surface of MPL. Then the gas diffusion electrodes were sintered at 350 °C in N_2 for 1 h. The electrodes were impregnated with 5 wt.% Nafion® solution by a spray technique. In the electrodes, the loading of Pt and Nafion in dry state was all about 0.4 mg cm^{-2}. The electrodes prepared as mentioned above were served as cathodes.

The anodes were prepared with the same method using the commercial Pt/C catalyst (TKK Corp., Pt content is 46.4 wt.%). The Pt loading in anodes was 0.3 mg cm^{-2}.

The MEA was prepared by hot-pressing the cathode, Nafion 212 membrane, and the anode at 140 °C and 1 MPa for 1 min. The effective area of the electrode was 5 cm^2. The MEA was mounted in a single cell with stainless steel end plates and stainless steel mesh flow fields as the current collectors.

2.3. Single cell test

The performance of the fuel cell was evaluated at a cell temperature of 80 °C. Hydrogen and oxygen were humidified before entering the cell, and were employed as the fuel and the oxidant, respectively. The humidification temperatures for hydrogen and oxygen were 90 and 85 °C, respectively. Both the pressure of hydrogen and oxygen were 0.2 MPa. Before the steady-state polarization curves were recorded, the cell was kept at a constant current density of 1000 mA cm^{-2} for about 6 h until the output voltage of the cell was stable.

2.4. Electrochemical accelerating aging test

Two kinds of AATs were performed by employing the CV measurement. One kind of AATs was to employ a three-electrode cell, in which a thin film electrode fabricated with Nafion solution (DuPont, USA) and the home-made Pt/C or $Pt/TiO_2/C$ catalyst on the surface of a glassy-carbon (GC) electrode was served as the working electrode, a Pt foil with the surface area of 3 cm^2 and a saturated calomel electrode (SCE) were used as the counter and the reference electrodes, respectively. The CV tests were performed in the potential range of −0.25 to +1.0 V for 1000 cycles in a N_2 saturated 0.5 mol L^{-1} H_2SO_4 solution at room temperature. The CV curves were recorded to calculate the electrochemical active surface area (EAS) of Pt in the catalysts by using the following equation [29]:

$$\mathrm{EAS} = \frac{Q_H}{Q_{ref} L_{Pt}}$$

in which Q_H is the charge of hydrogen adsorption; Q_{ref} is the charge for a monolayer adsorption of hydrogen on polycrystalline Pt, whose value is 210 C (cm^2 Pt)$^{-1}$; and L_{Pt} is the loading of Pt in the cathode.

The other kind of AATs was performed by measuring the CV curves of the cathode in a PEMFC single cell. In this case, the anode side was fed with hydrogen and served as the reference and counter electrodes. The cathode side was fed with nitrogen and served as the working electrode. The AATs were performed by employing the potential sweeping test in the range of +0.6–1.2 V for 3000 cycles. The EAS of Pt in the catalyst can be calculated as described above. In this experiment, the cell temperature was 80 °C, and the humidification temperature of hydrogen and nitrogen was 90 and 85 °C, respectively.

The CV measurements were performed using a CHI 625A electrochemical workstation (Chenhua Instrument Co., Shanghai, China).

2.5. Characterization of catalysts

XRD patterns of the catalyst were conducted on a PAN-analytical powder diffraction-meter (Philips X'Pert PRO) using Ni-filtered Cu Kα radiation (λ = 1.54056 Å) for the characterization of the crystalline structures of Pt and TiO_2.

The morphologies of the catalysts before and after the AAT were investigated by using transmission electron microscope (JEOL JEM-2011). The catalysts after the AAT were collected from the used cathode and were mixed with ethanol to form homogenous slurry ultrasonically. At least 200 metal particles were calculated to obtain the particle distribution diagram of each catalyst sample. The mean particle diameter (d_m) was calculated using the following formula [30]:

$$d_m = \frac{\sum_i n_i d_i}{\sum_i n_i}$$

in which n_i is the number of particles with the diameter d_i.

The bulk contents of Pt and Ti in the prepared $Pt/TiO_2/C$ catalyst were analyzed by ICP (Plasma-spec-ii, Leeman, USA).

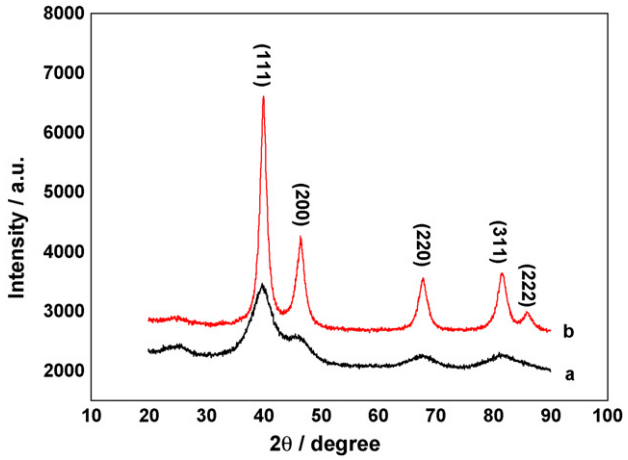

Fig. 1. XRD patterns of (a) Pt/C and (b) Pt/TiO_2/C catalyst.

3. Results and discussion

3.1. ICP measurement and XRD spectrum

The results obtained from ICP indicate that the content of Pt and Ti in Pt/TiO_2/C catalyst was 40 and 1.08 wt.%, respectively. Thus, the overall molar ratio was Pt:Ti = 9:1.

The XRD patterns of Pt/TiO_2/C and Pt/C catalyst are shown in Fig. 1. The Pt/TiO_2/C catalyst exhibited well-shaped characteristic peaks for the cubic crystalline platinum at 39°, 46°, 68°, 81° and 85°, corresponding to Pt (1 1 1), (2 0 0), (2 2 0), (3 1 1) and (2 2 2) plane, respectively. The Pt/C catalyst showed poorly defined peaks of Pt. The peak at the Bragg angle of 85° corresponding to Pt (2 2 2) plane cannot be observed from the XRD pattern of Pt/C. It can be concluded that the particle size of Pt/TiO_2/C is larger than that of Pt/C due to the heat-treatment of the Pt/TiO_2/C catalyst. Besides, no peak related to TiO_2 phases in Pt/TiO_2/C catalyst can be observed from Fig. 1. The reason might be the very low content of titanium (about 1.08%) in Pt/TiO_2/C catalyst. In addition, there is no shift in any of the diffraction peaks of Pt in Pt/TiO_2/C catalyst, which indicates that the addition of TiO_2 does not change the crystalline lattice of Pt.

3.2. Long-term durability of catalysts

The CV curves obtained with the thin film electrodes fabricated with Pt/C and Pt/TiO_2/C catalysts are shown in Fig. 2(a) and (b), respectively. The CV curves present the well-shaped current peaks corresponding to the adsorption/desorption of hydrogen at Pt surface, and the oxidation/reduction of the oxygen-containing species at Pt surface. The EAS of Pt in the catalyst is calculated as described in Section 2.2. The results are listed in Table 1. The initial EAS value of Pt in Pt/C catalyst before the AAT was 74.38 m^2 $(g\,Pt)^{-1}$, which was larger than that of Pt in Pt/TiO_2/C catalyst (64.52 m^2 $(g\,Pt)^{-1}$). The reduction of EAS value of Pt in Pt/TiO_2/C catalyst might be caused by the heat-treatment of the catalyst at 500 °C. After the potential sweep test in the range of −0.25 to +1.0 V for 1000 cycles, the EAS value of Pt in Pt/C reduced to 31.68 m^2 $(g\,Pt)^{-1}$. The remaining EAS of Pt in Pt/C after the AAT is about 42.6%. In contrast, the EAS of Pt in Pt/TiO_2/C catalyst was 48.81 m^2 $(g\,Pt)^{-1}$ after the AAT, which was obviously larger than that of Pt in Pt/C catalyst. The remaining EAS of Pt in Pt/TiO_2/C is about 75.6%. The results indicate that Pt/TiO_2/C catalyst is more durable than Pt/C catalyst.

Table 1
Electrochemical active surface area (EAS) of Pt/C and Pt/TiO_2/C catalyst.

Catalyst	EAS before AAT (m^2 $(g\,Pt)^{-1}$)	EAS after AAT (m^2 $(g\,Pt)^{-1}$)	EAS remaining
Pt/C	74.38	31.68	42.6%
Pt/TiO_2/C	64.52	48.81	75.6%

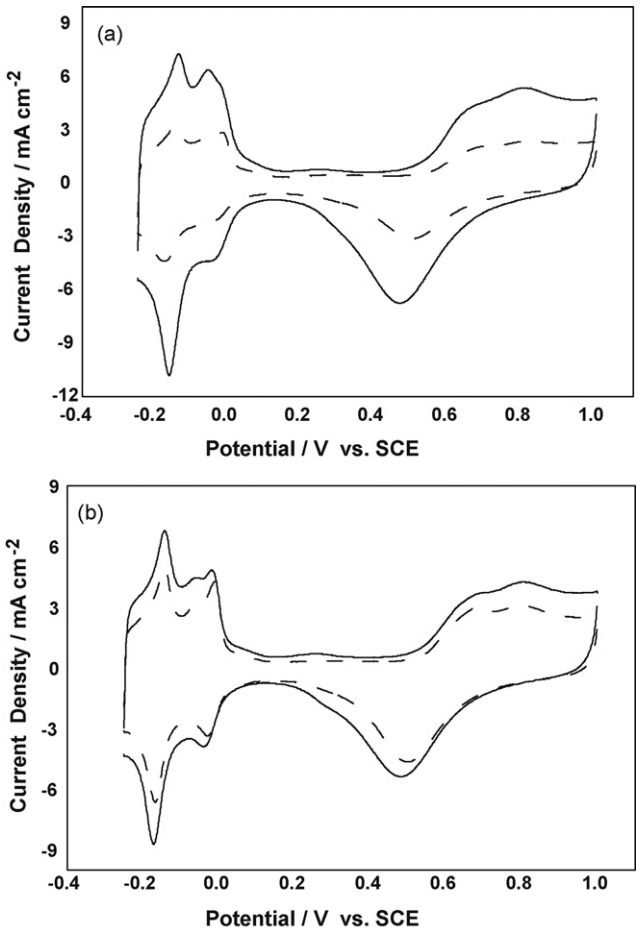

Fig. 2. Cyclic voltammograms obtained with the thin film electrodes fabricated with (a) Pt/C and (b) Pt/TiO_2/C catalyst in N_2-purged 0.5 mol L^{-1} H_2SO_4 solution before (solid line) and after (dash line) AAT. Potential scan rate: 50 mV s^{-1}.

Fig. 3 shows the polarization curves of oxygen reduction obtained with the thin film electrodes fabricated with the Pt/C and Pt/TiO_2/C catalysts. After the AAT, the half-wave potentials for oxygen reduction at Pt/C electrode and Pt/TiO_2/C electrode shifted negatively 58 and 14 mV, respectively. The apparent exchange current densities (i^0_{app}) of oxygen reduction were calculated from Tafel curves which is derived from the oxygen reduction polarization curves as shown in Fig. 3. The values were calculated to be 3.02×10^{-9} A cm^{-2} at Pt/C electrode before the AAT and 1.32×10^{-11} A cm^{-2} after the AAT, and 2.88×10^{-9} A cm^{-2} at Pt/TiO_2/C electrode before the AAT and 2.51×10^{-9} A cm^{-2} after the AAT. Although the initial value of i^0_{app} for oxygen reduction at Pt/C electrode was larger than that at Pt/TiO_2/C electrode, it reduced sharply from 3.02×10^{-9} to 1.32×10^{-11} A cm^{-2} after the AAT. On the contrary, the i^0_{app} of oxygen reduction at Pt/TiO_2/C electrode remained quite stable. It can be seen that the durability of the catalytic activity of Pt/TiO_2/C catalysts toward ORR is better than that of Pt/C catalysts.

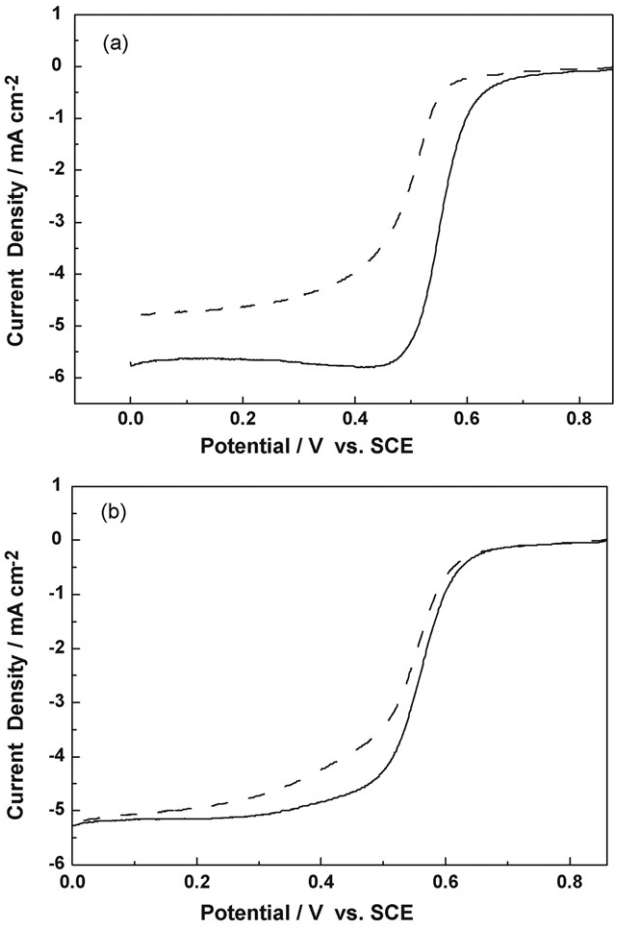

Fig. 3. Polarization curves of oxygen reduction at (a) Pt/C and (b) $Pt/TiO_2/C$ catalyst in O_2-saturated 0.5 mol L^{-1} H_2SO_4 before (solid line) and after (dash line) AAT. Potential scan rate: 5 mV s^{-1}. Rotation speed: 2500 rpm.

It can be concluded from the experimental phenomena as mentioned above that the $Pt/TiO_2/C$ catalysts are more tolerant to the AAT, which leads to the larger remaining EAS value and the higher durability of ORR activity after the AAT.

3.3. Long-term durability of catalysts in PEMFC

The long-term durability of the $Pt/TiO_2/C$ catalyst was investigated when it served as PEMFC cathode catalyst. Meanwhile, the long-term durability of the Pt/C catalyst as the PEMFC cathode catalyst was also investigated for comparison. At first, *I–V* curve of the single cell was measured before the AAT. Then the cathode was fed with nitrogen and the potential sweep test was performed from +0.6–1.2 V for 3000 cycles. Afterwards, the cathode was fed with oxygen again and *I–V* curve of the single cell was tested. The degradation rate of the single cell can be calculated by using the equation [31]:

$$\text{Degradation rate (mV/cycle)} = \frac{\text{final performance (mV)} - \text{original performance (mV)}}{\text{cycle number}}$$

I–V curves obtained with the single cells employing the Pt/C and $Pt/TiO_2/C$ cathode catalysts are shown in Fig. 4. It can be seen, the initial performance of the cell using the Pt/C cathode catalysts was slightly better than that of the cell using the $Pt/TiO_2/C$ catalysts. However, after the AAT, the performance of the cell using the

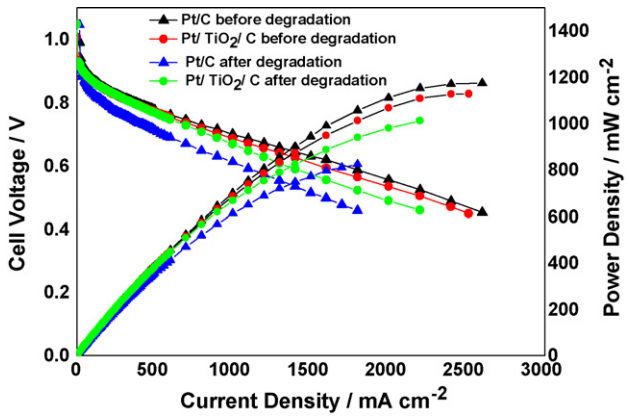

Fig. 4. Performances of PEMFC single cells. $P_{H_2} = P_{O_2} = 0.2$ MPa; $T_{cell} = 80\,^{\circ}C$; $T_{a,humi} = 90\,^{\circ}C$; $T_{c,humi} = 85\,^{\circ}C$.

$Pt/TiO_2/C$ catalysts was much better than that of the cell using the Pt/C catalysts. For example, after the AAT, the voltage loss of the cell using the $Pt/TiO_2/C$ catalysts at 200 mA cm^{-2} was about zero, while the value for the cell using the Pt/C catalysts was about 50 mV and the overall decay rate was 0.0167 mV $cycle^{-1}$. Similarly, the voltage loss of the cell using the $Pt/TiO_2/C$ at 1000 mA cm^{-2} was 18 mV (the overall decay rate was 0.006 mV $cycle^{-1}$), which was much lower than that of the cell using the Pt/C (88 mV and 0.0293 mV $cycle^{-1}$, respectively).

The voltage losses of the single cells caused by the AAT are recorded with respect to the operating current densities (Fig. 5). The voltage loss of the cell using the Pt/C catalysts was much larger than that of the cell using the $Pt/TiO_2/C$ catalysts at the same operating current densities. At the current densities less than 300 mA cm^{-2}, there was no voltage loss could be observed with the cell using the $Pt/TiO_2/C$ catalysts. On the contrary, the voltage loss of the cell using the Pt/C catalysts increased sharply to 44.6 mV when the operating current density increased from 0 to 100 mA cm^{-2}. The voltage loss of a PEMFC single cell at low current densities is considered to be caused by the low catalytic activities of the electrode (catalyst). Thus, it can be concluded that the catalytic activity of the Pt/C was reduced obviously by the AAT. On the contrary, the catalytic activity of the $Pt/TiO_2/C$ was almost unchanged. When the current densities were larger than 300 mA cm^{-2}, the voltage decrements of both the

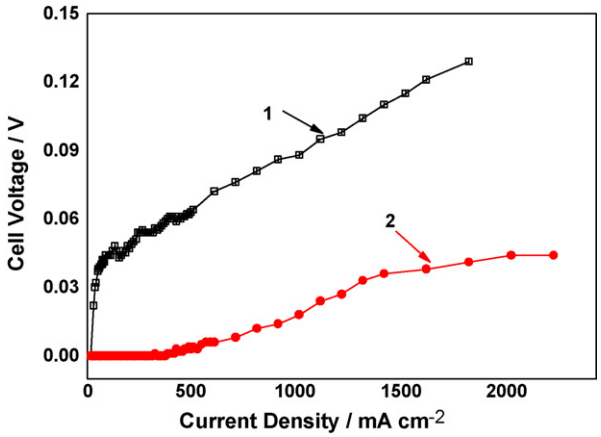

Fig. 5. The voltage losses of PEMFC single cells after AAT. Curve 1: cell using Pt/C cathode catalyst. Curve 2: cell using $Pt/TiO_2/C$ cathode catalyst.

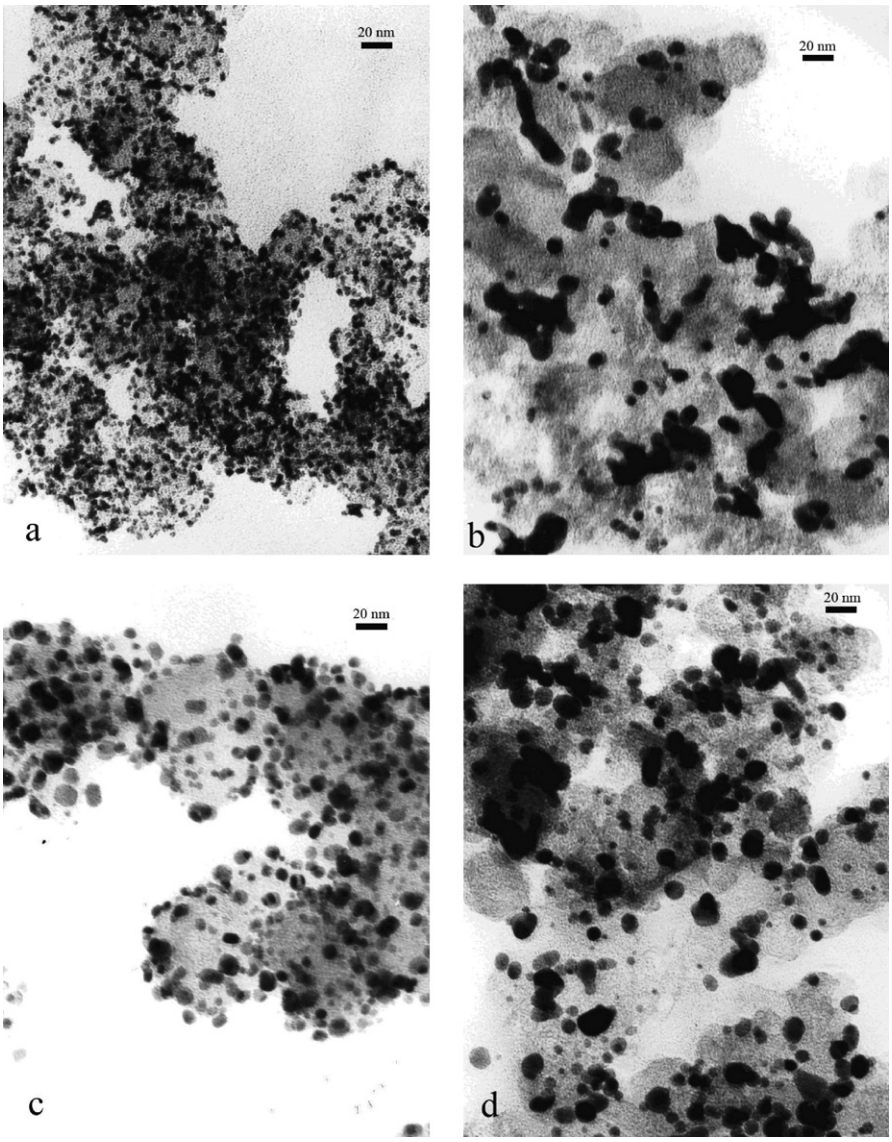

Fig. 6. TEM images of the catalysts: Pt/C catalyst (a) before AAT; (b) after AAT; $Pt/TiO_2/C$ catalyst (c) before AAT; and (d) after AAT.

cells increased obviously with the increase of the operating current densities. The increase of the voltage losses of the cell at higher current densities is caused by the increase of the inner resistance of the cell. This indicates that the inner resistances of the single cells using Pt/C and $Pt/TiO_2/C$ catalyst were increased obviously by the AAT.

The EAS values of Pt in the cathodes were also measured from the CV curves as described in Section 2.2. It showed that after the AAT, the reduction of EAS value of Pt in the $Pt/TiO_2/C$ catalysts was about 29.8% and was obviously less than the reduction of EAS value of 74.9% for the Pt in the Pt/C catalysts. The results show that the $Pt/TiO_2/C$ catalyst is more stable than Pt/C catalyst to the AAT.

The morphologies of the cathode catalysts before and after the AAT were observed and recorded using TEM. The TEM images and the distributions of Pt particle size are shown in Figs. 6 and 7, respectively. The results indicate that the dispersion of Pt particles in both the Pt/C and the $Pt/TiO_2/C$ catalysts was uniform before the AAT. The mean particle size was around 5.3 nm for Pt/C catalysts and 7.3 nm for $Pt/TiO_2/C$ catalysts. Thus, the Pt particle size in the $Pt/TiO_2/C$ catalysts was slightly larger than that in the Pt/C catalysts due to the heat-treatment of $Pt/TiO_2/C$ at 500 °C. After the AAT, the obvious agglomeration and coalescence of Pt particles in the Pt/C ctalysts were observed (as shown in Fig. 6(b)). The mean particle size of Pt increased to 26.5 nm with a broad size distribution. But for the $Pt/TiO_2/C$ catalysts, after the AAT the mean particle size of Pt increased to 9.2 nm, which was much smaller than the value of Pt in the Pt/C catalysts. Besides, the size distribution of Pt particles in the $Pt/TiO_2/C$ catalysts remained approximately uniform. It can be concluded that the long-term durability of the morphology of the $Pt/TiO_2/C$ is much better than that of the Pt/C when they are served as PEMFC cathode catalysts.

The improved stability and durability of the catalysts are possibly due to the existence of titanium oxide. The similar phenomena have been observed from the other transition metal oxide in the carbon-supported platinum catalysts [32]. However, the detailed mechanism of the metal oxide in the improvement of carbon support Pt catalysts is not clear now. The further investigation is under way.

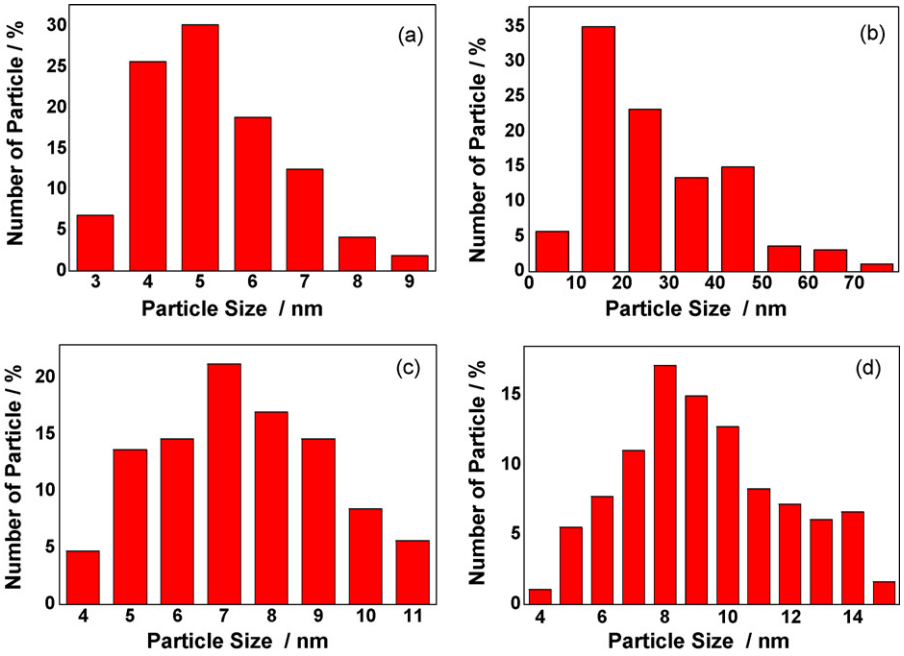

Fig. 7. Histograms of particle size distributions of the catalyst. Pt/C catalyst: (a) before AAT; (b) after AAT, Pt/TiO_2/C catalyst; (c) before AAT; and (d) after AAT.

4. Conclusions

Pt/TiO_2/C and Pt/C were prepared with a two-step reaction method and were employed as PEMFC cathode catalysts. After the AAT, the reduction of EAS value for the Pt/C catalysts was 74.96%, was significantly larger than the value of 29.79% for the Pt/TiO_2/C catalysts. The output voltage decrease of the single cell using the Pt/C catalysts was also larger than that of the cell using the Pt/TiO_2/C catalysts.

The obvious agglomeration and coalescence of Pt particles in the Pt/C catalysts caused by the AAT were observed from the TEM images. The mean particle size of the Pt in the Pt/C increased from 5.3 to 26.5 nm with a broad size distribution. But for the Pt/TiO_2/C catalyst, the mean particle size of the Pt increased from 7.3 to 9.2 nm after the AAT, which was much smaller than that of the Pt in the Pt/C catalysts.

In brief, the stability and long-term durability of PEMFC cathode catalysts are obviously improved by introducing TiO_2 into the catalysts.

Acknowledgements

Authors thank Ms. Yuanwei Ma and Mr. Yi Zou for the helpful discussions.

References

[1] A.K. Shukla, P.A. Christensen, A. Hamnett, M.P. Hogarth, J. Power Sources 55 (1995) 87.
[2] P.J. Ferreira, G.J. La O', Y. Shao-Horn, D. Morgan, R. Makharia, S. Kocha, H.A. Gasteiger, J. Electrochem. Soc. 152 (2005) A2256.
[3] E. Antolini, J. Mater. Sci. 38 (2003) 2995.
[4] Z. Siroma, K. Ishii, K. Yasuda, Y. Miyazaki, M. Inaba, A. Tasaka, Electrochem. Commun. 7 (2005) 1153.
[5] L. Li, Y.C. Xing, J. Electrochem. Soc. 153 (2006) A1823.
[6] Y.Y. Shao, G.P. Yin, Y.Z. Gao, P.F. Shi, J. Electrochem. Soc. 153 (2006) A1093.
[7] K.F. Blurton, H.R. Kunz, D.R. Rutt, Electrochim. Acta 23 (1978) 183.
[8] Y.F. Zhai, H.M. Zhang, D.M. Xing, Z.G. Shao, J. Power Sources 164 (2007) 126.
[9] A. Honji, T. Mori, K. Tamura, Y. Hishinuma, J. Electrochem. Soc. 135 (1988) 355.
[10] M. Watanabe, K. Tsurumi, T. Mizukami, T. Nakamura, P. Stonehart, J. Electrochem. Soc. 141 (1994) 2659.
[11] H.R. Colon-Mercado, H. Kim, B.N. Popov, Electrochem. Commun. 6 (2004) 795.
[12] P. Yu, M. Pemberton, P. Plasse, J. Power Sources 144 (2005) 11.
[13] Z.D. Wei, H.T. Guo, Z.Y. Tang, J. Power Sources 62 (1996) 233.
[14] K.T. Kim, Y.G. Kim, J.S. Chung, J. Electrochem. Soc. 142 (1995) 1531.
[15] W. Roh, J. Cho, H. Kim, J. Appl. Electrochem. 26 (1996) 623.
[16] D.A. Landsman, F.J. Luczak, in: W. Vielstich, A. Lamm, H.A. Gasteiger (Eds.), Handbook of Fuel Cells: Fundamentals, Technology, and Applications, vol. 4, John Wiley & Sons, New York, 2003 (Chapter 60).
[17] D. Thompsett, in: W. Vielstich, A. Lamm, H.A. Gasteiger (Eds.), Handbook of Fuel Cells: Fundamentals, Technology, and Applications, vol. 3, John Wiley & Sons, New York, 2003 (Chapter 37).
[18] T. Toda, H. Igarashi, H. Uchida, M. Watanabe, J. Electrochem. Soc. 146 (1999) 3750.
[19] T. Toda, H. Igarashi, M. Watanabe, J. Electrochem. Soc. 460 (1999) 258.
[20] E. Antolini, J.R.C. Salgado, E.R. Gonzalez, J. Power Sources 160 (2006) 957–968.
[21] G. Liu, H.M. Zhang, H.X. Zhong, J.W. Hu, D.Y. Xu, Z.G. Shao, Electrochim. Acta 51 (2006) 5710.
[22] G. Liu, H.M. Zhang, Y.F. Zhai, Y. Zhang, D.Y. Xu, Z.G. Shao, Electrochem. Commun. 9 (2007) 135.
[23] D.S. Kim, S.Y. Kwak, Appl. Catal. A: Gen. 323 (2007) 110–118.
[24] S. Sathiyanarayanan, S. Syed Azim, G. Venkatachari, Electrochim. Acta 52 (2007) 2068.
[25] J. Shim, C.R. Lee, H.K. Lee, J.S. Lee, E.J. Cairns, J. Power Sources 102 (2001) 172.
[26] L. Xiong, A. Manthiram, Electrochim. Acta 49 (2004) 4163.
[27] H. Ekstroem, B. Wickman, M. Gustavsson, P. Hanarp, L. Eurenius, E. Olsson, G. Lindbergh, Electrochim. Acta 52 (2007) 4239.
[28] M. Gustavsson, H. Ekstrom, P. Hanarp, L. Eurenius, G. Lindbergh, E. Olsson, B. Kasemo, J. Power Sources 163 (2007) 671.
[29] X.L. Wang, H.M. Zhang, J.L. Zhang, H.F. Xu, Z.Q. Tian, J. Chen, H.X. Zhong, Y.M. Liang, B.L. Yi, Electrochim. Acta 51 (2006) 4909.
[30] I. Dobrosz, K. Jiratova, V. Pitchon, J.M. Rynkowski, J. Mol. Catal. A: Chem. 234 (2005) 187.
[31] J. St-Pierre, J. Roberts, K. Colbow, S. Campbell, A. Nelson, J. N. Mater. Electrochem. Syst. 8 (2005) 163.
[32] W.M. Chen, G.Q. Sun, J.S. Guo, X.S. Zhao, S.Y. Yan, J. Tian, S.H. Tang, Z.H. Zhou, Q. Xin, Electrochim. Acta 51 (2006) 2391.